NOTICE CONCERNING COPYRIGHT RESTRICTIONS

This document may contain copyrighted materials. These materials have been made available for use in research, teaching, and private study, but may not be used for any commercial purpose. Users may not otherwise copy, reproduce, retransmit, distribute, publish, commercially exploit or otherwise transfer any material.

The copyright law of the United States (Title 17, United States Code) governs the making of photocopies or other reproductions of copyrighted material.

Under certain conditions specified in the law, libraries and archives are authorized to furnish a photocopy or other reproduction. One of these specific conditions is that the photocopy or reproduction is not to be "used for any purpose other than private study, scholarship, or research." If a user makes a request for, or later uses, a photocopy or reproduction for purposes in excess of "fair use," that user may be liable for copyright infringement.

This institution reserves the right to refuse to accept a copying order if, in its judgment, fulfillment of the order would involve violation of copyright law.

Geothermal Resources Council Transactions, Vol. 28, August 29 - September 1, 2004

Geothermal Resource Mapping Using Teleseismic Conversions

Charles K. Wilson[1] and Craig H. Jones[2]

[1]Stanford University, Department of Geophysics
[2]University of Colorado, Boulder and CIRES

ABSTRACT

We adapt an existing seismic imaging tool that exploits converted phases generated in the lithosphere by teleseismic earthquakes to seismically map geothermal resource geometry and potential. Application of this technique to the Coso geothermal field near Ridgecrest, California reveals a shallow, well-defined region of low seismic wavespeed beneath the modern geothermal field. Most likely this body represents the top of a zone of partial melt based on the amplitude of the converted phase and its position beneath the field. Depth migration of converted phases from all recorded events allows us to create a volume of seismic impedance of the entire crust from which we infer the relationship of the shallow partial melt to regional extension.

Introduction

Resource exploitation in producing geothermal fields can be enhanced with improved knowledge of resource geometry inferred from seismic images. But, obtaining an accurate, well-resolved, image of the subsurface beneath active geothermal fields can be difficult. Traditional exploration seismology techniques suffer from high seismic attenuation and large seismic wavespeed variations related to the highly deformed and thermally altered material present in geothermal areas. Considering the difficulties in obtaining images of the upper few kilometers, creating interpretable images of the middle and lower crust of active geothermal areas is nearly impossible. Recognizing the shortcomings within geothermal areas of otherwise successful reflection seismology experiments, we have applied an existing seismic technique which exploits locally scattered waves generated by im-

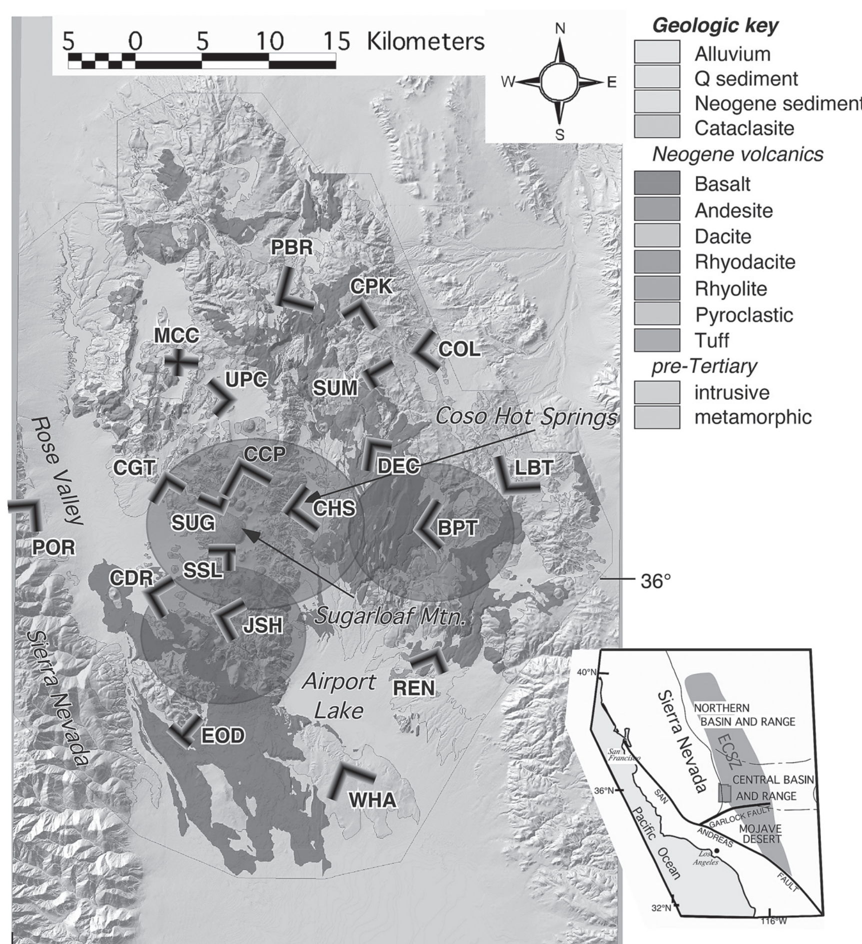

Figure 1. Shaded relief map with geology centered on Coso geothermal area shown with a southwestern United States tectonic sketch to the right. The box on the tectonic map indicates the location of the study area. The black lines on the map represent the location of three-component seismometer arrays used in the seismic imaging study. The larger transparent circle centered on Sugarloaf Mountain shows the horizontal extent of the imaged partial melt region while the small peripheral circles show the inferred extent of mid-crustal seismic anisotropy inferred to be the locations of a sub-horizontal shear zone accommodating strain variations between the upper and lower crust.

pinging teleseismic earthquakes (30°-60° epicentral distance) to image the crust and upper mantle beneath Coso geothermal field. We show application of this imaging technique at Coso and demonstrate our ability not only to map the heat source of the geothermal field in detail but also provide information about the tectonic environment where the field resides to assist with resource development.

Experiment Design and Data Analysis

We recorded ~220 Gb of 40 samples per second, three-component seismograms in and around the Coso Geothermal Area from November 1998 to May 2000 [*Wilson et al.*, 2003]; most of the data is available from the IRIS Data Management Center (http://www.iris.washington.edu). With over 150 sites within an area of ~700 km^2, this is one of the densest portable, passive seismic deployments to date (Figure 1). We examined over 220 high quality teleseismic events to exploit P-to-S conversions within the shallow lithosphere [*Burdick and Langston*, 1977; *Phinney*, 1964] in an effort to map crustal variations in seismic impedance. For each chosen earthquake recorded by each dense array, we apply a linear moveout correction to align the incoming P waves at each station on each component. The seismograms are then stacked to cancel energy not traveling in the same direction as the incoming teleseismic arrivals. This technique enhances P-to-S conversion in the lithosphere while canceling near surface arrivals due to topography or velocity heterogeneity. Stacking in this manner allows the use of higher frequency portions of the teleseismic wavefield that are usually contaminated by near surface scattering thereby improving the overall imaging capabilities of this method. After stacking, the horizontal seismograms are rotated into an event based radial/transverse reference frame followed by deconvolution using the vertical component as the source function. The fully processed horizontal seismograms now represent arrivals of lithospheric P-to-S conversions.

Assuming a seismic wavespeed structure for the crust and upper mantle within the study area, we can project the recorded converted waves back to their loci of generation to create a three dimensional volume of converted wave amplitude that represents shear modulus variations. This tool is very effective at mapping discontinuities in material properties such as those found at the Moho or between normal crust and regions of partial melt.

Crustal Structure

An important converted arrival observed by Wilson et al. [2003] was a high-amplitude negative polarity arrival from near 5 km depth generated from the top of a low wavespeed zone (Figure 2). The low wavespeed zone appears to be confined below the recent rhyolite domes within the modern geothermal area. Based on forward modeling with synthetic seismograms, the magnitude of the velocity decrease was shown to be ~30%. A velocity contrast of this magnitude suggests the presence of partial melt (Figure 3) with melt percentages possibly as high as 30% [*Wilson et al.*, 2003] depending on the melt composition and melt texture.

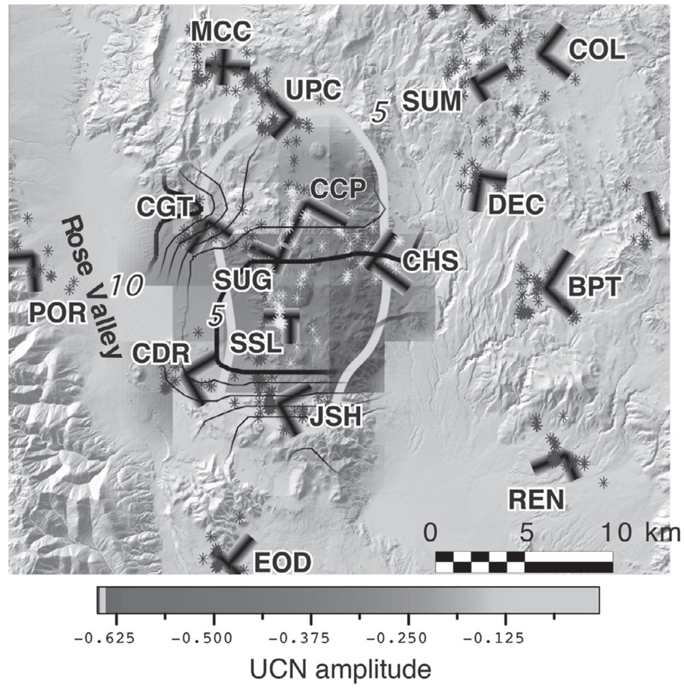

Figure 2. Character and extent of the top of the shallow low wavespeed zone from the calculated converted wave amplitude volume. Darkened blocks indicate the amplitude of the converted arrivals from the top of the low wavespeed zone; depth of conversion is contoured in kilometers below sea level for the regional velocity structure. Stars represent piecing points of teleseismic rays at 5 km depth. Note increasing depth and increasing amplitude to the south and west possibly indicating structural control of the resource. The irregular surrounding the arrays JSH, SUG, CHS, and SSL separates rhyolite-dominant interior from basalt-dominant exterior. Coso Hot Springs is at the corner of the "L" of the CHS array.

In addition to the region of shallow partial melt, we also recorded arrivals from the Moho and a mid-crustal interface. The Moho appeared to be flat and near 30 km depth below sea level throughout the study area (Figure 3) as has been reported for much of the Basin and Range province [e.g. as summarized by Gans, 1987]. The mid-crustal arrival generated near 16 km depth shows considerably more variability. The amplitude decreases and depth increases for this conversion beneath the shallow low wavespeed zone. It appears to be strongest, and clearest just off the edge of the partial melt region (Figure 3).

Interpretation of the Mid-Crustal Feature

The close spatial relationship of the mid-crustal feature with the magma body suggests that they are related. These could be basaltic sills, which would produce seismically isotropic conversions. Alternatively, the mid-crustal converter could be a shear zone, with the magnitude of shear decreasing away from the magma body and would most likely be anisotropic. The development of the shear zone would be a result of strain accommodation through crust with dramatic variation in strength. A region of partial melt imbedded in the upper crust would lead to large local viscosity variations, which we expect would localize upper crustal strain within the low viscosity region. The strain localization leads to an increase in hori-

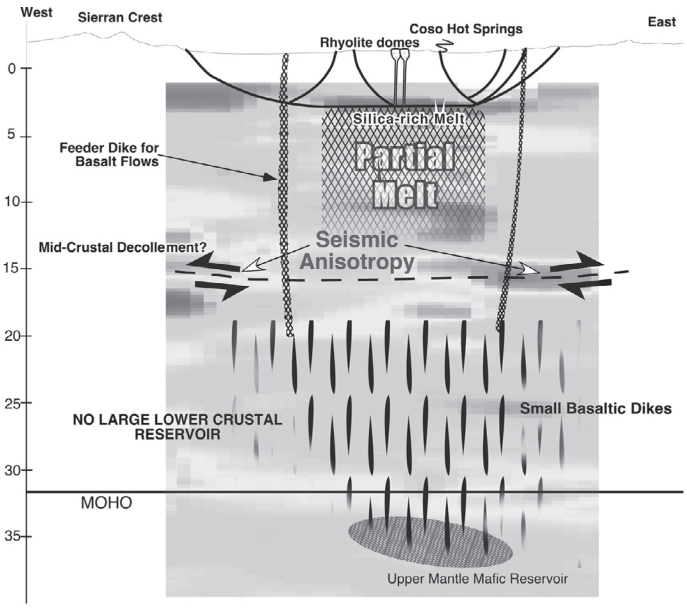

Figure 3. Cartoon showing structure of the Coso geothermal field and the possible relationship between the shallow magma body and regional tectonic features. A common conversion point stacked image made from teleseismic earthquake rays illustrates the Moho, a mid crustal discontinuity, and the shallow magma body. The magma body may act as a strain guide for deformation in the mid to upper crust. Coupled with lower crustal flow this area may accommodate a significant amount of strain.

zontal velocities adjacent to the low viscosity region relative to the lower crust. If the vertical strain gradient and total strain are large enough, accommodation of the relative motion will require the development of a mid crustal shear zone.

Shear zones provide a very effective means to create seismic anisotropy within crustal rocks[*Godfrey et al.*, 2000]. Several studies have demonstrated the usefulness of crustal conversions in locating crustal seismic anisotropy [*Jones and Phinney*, 1998; *Levin and Park*, 1997; *McNamara and Owens*, 1993]. Anisotropic material above a conversion interface produces variations with back-azimuth of arrival time and conversion amplitude resulting from the directional dependence of elastic properties within anisotropic material.

To test our hypothesis of melt induced strain localization, we use synthetic seismograms to demonstrate the presence (or absence) of seismic anisotropy at the mid-crustal converter south of the Coso low wavespeed zone recorded by array JSH (see Figure 1 for array location). The negative polarity conversion observed on the JSH radial receiver functions just after 1 s indicate the presence of a rapid decrease in wavespeed with depth

Table 1. Best synthetic model for the JSH array. Results are shown in Figure 3.

Z (m)	Density	Vp	Vs	% Vp anis.	%Vs anis.	Trend	Plunge	Strike	Dip
13000	2700	5500	3400	-	-	0	0	0	0
200	2600	5000	2500	-	-	0	0	0	0
6500	2700	6000	3100	-	-	0	0	300	30
1000	2750	6000	3100	20	20	280	25	0	0
13000	2800	6600	3800	-	-	0	0	0	0
-	2550	8000	4800	-	-	0	0	0	0

(Table 1). The associated energy near the same time on the transverse receiver functions indicates the interface dips to the north-northeast towards the region of partial melt (Figure 4; Table 1). The arrival from near 3 s shows large variations in arrival time with back-azimuth. We find the pattern of arrival time variations difficult to match without the dipping interface located at the base of the low speed zone (Figure 4) or a plunging axis of symmetry within a mid-crustal anisotropic region.

Conclusions

We have demonstrated that with proper array design, the teleseismic wavefield may be processed to produce medium resolution converted wave images of the entire crust beneath geothermal fields. In the case of Coso we have shown that with sufficiently dense array spacing, thermal anomalies of reasonable magnitudes may be mapped with vertical and horizontal resolution on the order of 1 km or less. In addition, this technique provides a straight forward means to incorporate information from seismic anisotropy, which may be helpful in understanding the shallow reservoir as well as local tectonic structures. Attesting to the usefulness of this technique in resource mapping, the Coso Geothermal Programs Office has purchased several instruments to fill in data gaps from the initial experiment and to continue ongoing reservoir monitoring efforts.

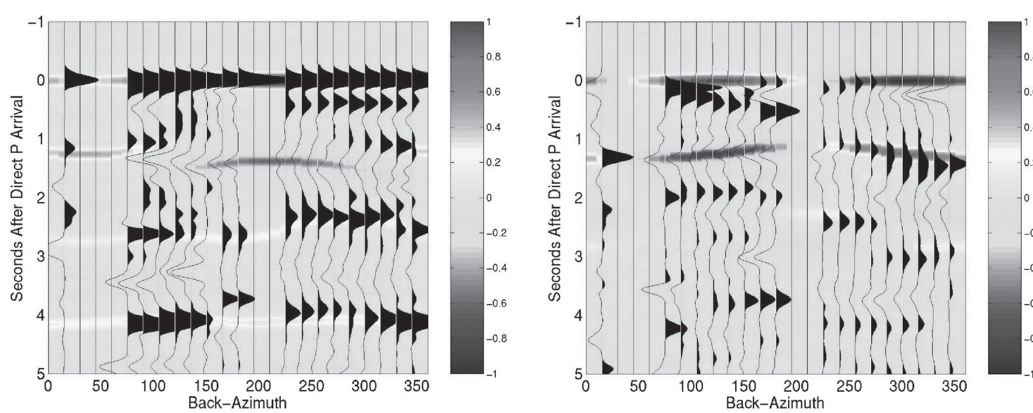

Figure 4. Plot showing radial and transverse synthetic receiver functions for our best fit model compared to processed receiver functions recorded just to the south of the partial melt region (array JSH on Figure 1). The left hand column shows radial receiver functions plotted in time and stacked by back-azimuth. The grey plot behind shows calculated synthetics for the model described in Table 1. The right hand column shows the associated recorded and calculated synthetic transverse receiver functions. Model (a) has a shallow low wavespeed zone overlying a mid crustal layer of anisotropy. The best-fit model requires both the dipping low velocity layer and a thin layer of mid crustal anisotropy to explain the observations.

Future Work

At the present, work is underway at Stanford University to incorporate imaging schemes based on wavefield continuation methods using the teleseismic wavefield [e.g. *Shragge and Artman*, 2003]. These methods allow easy incorporation of arbitrarily complex three-dimensional seismic wavespeed models that are capable of dealing with difficult multipathing that occurs within regions of extreme velocity heterogeneity. These techniques have been successfully applied in sub-salt imaging problems (directly analogous to sub-melt imaging) regularly encountered in oil exploration. With these types of advances on the horizon we may expect to combine active source, local earthquake sources, and teleseismic earthquake sources into a common imaging framework in the not too distant future.

References

Burdick, L.J., and C.A. Langston, Modeling Crustal Structure through Use of Converted Phases in Teleseismic Body-Wave Forms, *Bull. Seismol. Soc. Amer.*, *67*, 677-691, 1977.

Godfrey, N.J., N.I. Christensen, and D.A. Okaya, Anisotropy of Schists: Contribution of Crustal Anisotropy to Active Source Seismic Experiments and Shear Wave Splitting Observations, *J. Geophys. Res.*, *105*, 27991-28007, 2000.

Jones, C.H., and R.A. Phinney, Seismic Structure of the Lithosphere from Teleseismic Converted Arrivals Observed at Small Arrays in the Southern Sierra Nevada and Vicinity, California, *J. Geophys. Res.*, *103*, 10065-10090, 1998.

Levin, V., and J. Park, Crustal Anisotropy in the Ural Mountains Foredeep from Teleseismic Receiver Functions, *Geophys. Res. Lett.*, *24*, 1283-1286, 1997.

McNamara, D.E., and T.J. Owens, Azimuthal Shear-Wave Velocity Anisotropy in the Basin and Range Province Using Moho Ps Converted Phases, *J. Geophys. Res.*, *98*, 12003-12017, 1993.

Phinney, R.A., Structure of the Earth's Crust from Spectral Behavior of Long-Period Body Waves, *J. Geophys. Res.*, *69*, 2997-3017, 1964.

Shragge, J.C., and B.W. Artman, Wave-Equation Imaging of Teleseismic Body-Wave Coda, *EOS Trans. AGU, 84(46), Fall Meet. Suppl.*, *Abstract S11E-0335*, 2003.

Wilson, C.K., C.H. Jones, and H.J. Gilbert, Single-Chamber Silicic Magma System Inferred from Shear Wave Discontinuities of the Crust and Uppermost Mantle, Coso Geothermal Area, California, *J. Geophys. Res.*, *108*, art. no.-2226, 2003.